XXI Simposio CEA de Control Inteligente
24-26 de junio de 2026, Salamanca

Mejora de la Predicción Virtual de Temperatura en PEMFC mediante Modelado en Espacio de Estados con Optimización de Retardo.

Abiola, A O.*, Barragán A. J., Andújar, J M, Segura, F M.,
Centro de Investigación en Tecnología, Energía y Sostenibilidad (CITES), Universidad de Huelva, España

To cite this article: Abiola, A.O., Segura, F.M., Andújar, J.M., Barragán A. J.. 2026. Improving Virtual Temperature Prediction in PEM fuel cells Through Delay-Aware State-Space Modelling. XXI Simposio CEA de Control Inteligente, Salamanca (Spain), 2026.

Resumen

La refrigeración es una operación crítica en las pilas de combustible de membrana de intercambio protónico (PEMFC), ya que una temperatura excesiva puede reducir el rendimiento y comprometer la fiabilidad del sistema. El fallo de un sensor de temperatura dentro del circuito de refrigeración puede provocar una gestión térmica inadecuada. Cuando ocurre un fallo de sensor, la predicción mediante sensado virtual de la variable de proceso que ha fallado puede mejorar la tolerancia a fallos y la seguridad operativa. En este trabajo, la temperatura de salida del agente refrigerante se utiliza como caso de estudio representativo. Los sensores virtuales basados en modelos de espacio de estados suelen desarrollarse utilizando variables operativas medidas; sin embargo, la influencia de la selección de entradas y del retardo térmico sobre la precisión de predicción sigue siendo insuficientemente estudiada. Este trabajo evalúa diferentes combinaciones de variables predictoras y la optimización del retardo de entrada para la predicción virtual de temperatura en PEMFC mediante modelado en espacio de estados basado en Numerical Algorithms for Subspace State-Space System Identification (N4SID). Se utilizaron datos experimentales de corriente de pila, voltaje, temperatura de entrada del refrigerante y temperatura de salida del refrigerante para el desarrollo y validación de los modelos. Inicialmente se evaluaron múltiples combinaciones de entradas para establecer el rendimiento base de predicción, seguido de un barrido sistemático de retardos para identificar los retardos óptimos. Los resultados demuestran que una selección adecuada de entradas y la optimización del retardo mejoran significativamente la precisión de predicción al capturar los efectos de memoria térmica. La metodología propuesta proporciona un marco eficaz para mejorar el sensado virtual basado en el espacio de estados en pilas de combustible de tipo PEM.

Palabras clave: Pila de Combustible PEM, Sensor Virtual, Identificación en Espacio de Estados, Optimización del Retardo de Entrada, Dinámica Térmica, Monitorización Tolerante a Fallos

Improving Virtual Temperature Prediction in PEM fuel cells Through Delay-Aware State-Space Modelling

Abstract

Cooling is a critical operation in proton exchange membrane fuel cells (PEMFCs), as excessive temperature can reduce performance and compromise system reliability. Failure of a temperature sensor within the cooling loop may lead to improper thermal management. When a sensor fault occurs, prediction of the missing process variable through virtual sensing can improve fault tolerance and operational safety. In this study, outlet coolant temperature is used as a representative case study. State-space virtual sensors are commonly developed using measured operating variables; however, the influence of input selection and thermal delay on prediction accuracy remains insufficiently investigated. This study evaluates different predictor-variable combinations and input-delay optimization for PEMFC virtual temperature prediction using Numerical Algorithms for Subspace State-Space System Identification (N4SID). Experimental data comprising stack current, voltage, inlet coolant temperature, and outlet coolant temperature were used for model development and validation. Multiple input combinations were first assessed to establish baseline prediction performance, followed by a systematic delay sweep to identify optimal delays. Results demonstrate that appropriate input selection and delay optimization significantly improve prediction accuracy by capturing thermal-memory effects. The proposed methodology provides an effective framework for enhancing state-space virtual sensing in PEMFC systems.

Keywords: PEM Fuel Cell, Virtual Sensor, State-Space Identification, Input Delay Optimization, Thermal Dynamics, Fault-Tolerant Monitoring.

*Autor para correspondencia: abiodun.abiola@alu.uhu.es
Attribution-NonCommercial-ShareAlike 4.0 International (CC BY-NC-SA 4.0)

1. Introduction

Recent thermal-management studies in proton exchange membrane fuel cells (PEMFC) have mainly focused on cooling-system design, temperature regulation, and controller performance, while relatively limited attention has been given to virtual temperature sensing under sensor-failure conditions. (Deng et al., 2025) provided a comprehensive review of fuel-cell modelling, control, and optimization techniques, highlighting the importance of thermal management for fuel-cell performance and durability. The review classified existing approaches into physics-based thermal models, dynamic-system and state-space models, temperature-control strategies such as proportional–integral–derivative control, fuzzy logic, model predictive control, active disturbance rejection control, and adaptive control, as well as data-driven approaches including artificial neural networks, deep learning, long short-term memory networks, and deep reinforcement learning.

Although these approaches have contributed significantly to PEMFC thermal management, relatively few studies have investigated virtual temperature sensing and temperature prediction under sensor-fault conditions. (Huynh et al., 2026) developed a real-time internal-temperature monitoring framework based on inverse heat conduction and reduced-order modelling, while (Fuchs et al., 2025) proposed a nonlinear observer with an extended Kalman filter for estimating internal PEMFC temperature profiles.(Li et al., 2026) developed a deep-learning-based coolant-temperature prediction model using long short-term memory networks and XGBoost, demonstrating the importance of thermal inertia and delayed thermal responses in temperature prediction.

Owing to thermal inertia and coolant transport dynamics, PEMFC thermal systems inherently exhibit delayed input–output responses, meaning that changes in operating conditions may not be immediately reflected in the measured outlet temperature. Consequently, delayed inputs may contain valuable information for improving virtual temperature prediction. In the system-identification and observer-design literature, several studies have shown that delay estimation can significantly improve system representation and state estimation accuracy.(Drakunov et al., 2006) proposed observer-based delay identification methods for time-delay systems, while (Novella-Rodrìguez et al., 2019) and (Ingebretsen and Rotondo, 2022) demonstrated the importance of simultaneously estimating system states and input delays.

Despite these advances, the influence of predictor-variable selection and input-delay optimization on state-space virtual temperature sensing remains largely unexplored. This study addresses this gap by evaluating multiple input combinations and systematically investigating input-delay optimization within an N4SID-based framework for PEMFC virtual temperature sensing.

The remainder of this paper is organized as follows. Section 2 describes state-space modelling methodology, including the input-delay optimization procedure and the experimental set-up to acquire PEM fuel-cell dataset. Section 3 presents and discusses the prediction results obtained from different input configurations and delay settings. Finally, Section 4 summarizes the main conclusions and future research directions.

2. Methodology

To achieve the objectives of this study, state-space virtual temperature models were developed using experimental PEM fuel-cell data and identified using the Numerical Subspace State-Space System Identification (N4SID) algorithm. Stack current (I), stack voltage (V), and inlet cooling-water temperature (T_{in}) were considered as candidate predictor variables, while outlet cooling-water temperature (T_{out}) was selected as the target variable for virtual sensing. The selection of the input variables is premised on the fact that current is directly related to electrochemical heat generation while voltage reflects stack operating conditions and internal losses. In addition, Inlet coolant temperature represents the thermal boundary condition imposed by the cooling system. Multiple input-variable combinations, including individual variables and combined inputs, were first evaluated to establish baseline prediction performance and determine the influence of predictor selection on model accuracy. Subsequently, a systematic input-delay optimization procedure was applied to each input configuration to investigate the effect of thermal-memory behaviour on state-space prediction performance.

2.1. State space model (SSM)

The dynamic behaviour of the PEM fuel cell was represented using a discrete-time linear state-space model identified from experimental data. Although PEMFCs exhibit nonlinear behaviour, linear state-space models are widely used to represent the dominant dynamics around a specific operating region (Liu et al., 2025). Such models are attractive for real-time virtual sensing because of their low computational complexity and ease of implementation. The general discrete-time state-space formulation is given by (1) and (2).

$$x(k+1) = Ax(k) + Bu(k) \quad (1)$$
$$y(k) = Cx(k) + Du(k) \quad (2)$$

where:

- x represents the state vector,
- u represents the input vector,
- y represents the predicted output vector
- k represents sampling time
- A is the state-transition matrix describing the internal system dynamics,
- B is the input matrix describing the influence of the inputs on the states,
- C is the output matrix relating the states to the measured output,
- D is the direct feedthrough matrix representing direct input–output coupling.

The values of the state-space matrices A, B, C and D were determined from experimental data using the Numerical algorithms for Subspace State Space System Identification (N4SID) method (MathWorks, 2026).

At each sampling instant, the new state vector was updated using the previous state and current input values, after which the predicted outlet temperature was calculated from the estimated state vector.

2.2. Input delay Optimisation

Input delays have been shown to improve observer and state-estimation performance by providing a more accurate representation of system dynamics (Drakunov et al., 2006; Ingebretsen and Rotondo, 2022). Owing to the thermal inertia of PEMFC cooling systems, delayed input variables may contain information that is not immediately reflected in the outlet coolant temperature. Introducing this delay in the state space modelling of the fuel cell involves using past values of input data to predict the present outlet coolant temperature, thereby accounting for the delayed thermal response of the cooling system. Figure 1 illustrates the implementation of a one-second input delay, where the input variables are shifted by one time step before being used for model identification.

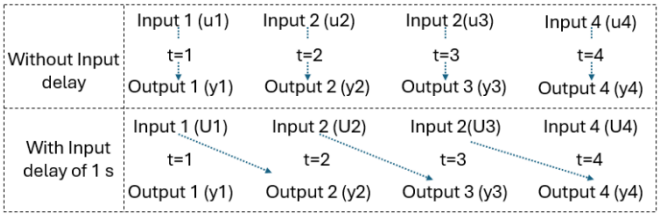


Figure 1: Schematic illustration of input delay in state-space modelling

Since the experimental data were sampled at 1 s intervals, input delays between 0 and 10 s were systematically evaluated in steps of 1 s within the N4SID modelling procedure. For each input configuration, a common delay was applied to all predictor variables. The delayed versions of the input variables were assessed for each input configuration, and the optimum delay was selected as the delay producing the lowest RMSE on the testing dataset. Before prediction with the test data, the initial state vector x (0) is initialized using the most recent measurements available before sensor failure.

2.3. Experimental Data Acquisition

Experimental data were collected from a PEMFC shown in Figure 2. Details of the set up are shown in Table 1. The fuel cell was operated using commercial dry hydrogen under dynamic loading conditions in order to generate varying thermal responses suitable for virtual temperature sensing analysis.

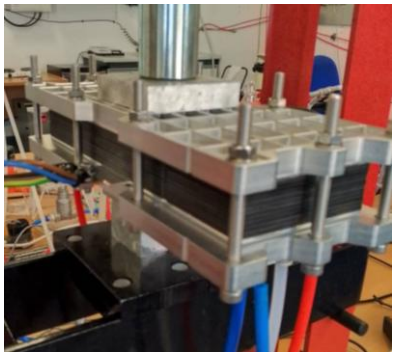


Figure 2: PEMFC stack used for data acquisition.

The experimental setup included measurement of stack current(I), voltage(V), inlet cooling-water temperature (T_{in}), and outlet cooling-water temperature (T_{out}). The operating condition of the stack follows the current demand with hydrogen inlet pressure between 0.2 and 0.4 bar, air inlet pressure between 0.1 and 0.2 bar, stack inlet air flow rate between 14 and 51 L/min, and air relative humidity between 70 and 80%.

Table 1: Experimental Set-up

Parameter	Value	Measurement Device
Number of Cells	10 cells	-
Active Area	220 cm^2	-
Air pressure	0.1 - 0.2 bar	Festo SFAB
Air flow	14 - 51 L/min	
Air Humidity	70 - 80%	Texense PTH CAN
Hydrogen Pressure	0.2 - 0.4 bar	Alicat M Series
Hydrogen Flow	0 – 16 slpm	
Hydrogen Humidity	0 % (dry hydrogen)	Trican HTD2800
Current	0 – 220 A	B&K 8415B
Voltage	0 to 10 V	
Temperature	22 to 60 °C	WIKA TF35

The PEMFC employed a closed-loop cooling circuit. During the experiments, cooling-water flow rate varied between 0.3125 and 3.17 L/min. A cooling fan was operated at minimum speed throughout the experiments to promote observable stack-temperature variations. No active fan-speed or radiator-control signal was included in the modelling framework. The observed thermal response was primarily driven by changes in stack current, while the coolant system regulated heat removal and prevented excessive temperature rise. Process data were acquired at a sampling interval of 1 s using LabVIEW® and a National Instruments USB-6218 data-acquisition device. These data were continuously recorded under transient operating conditions to generate datasets containing both electrical and thermal dynamic behaviour. This is shown in Figures 3 and Figure 4.

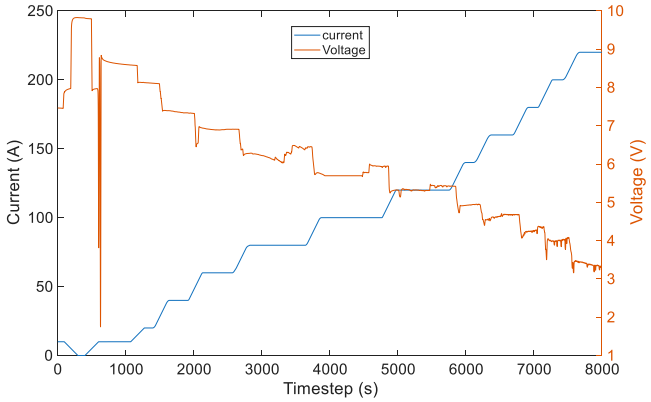


Figure 3: Experimental data showing variation of current and voltage.

Figure 4 shows the virtual sensing (testing) region used for model evaluation.

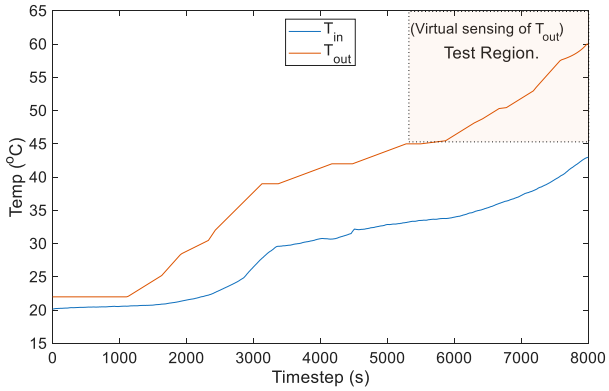


Figure 4: Experimental data showing variation of inlet and outlet cooling water temperature as well as the test region of T_{out}.

Although Tin varied smoothly, it covered approximately 22–43 °C and was accompanied by cooling-water flow variations between 0.3125 and 3.17 L/min, providing sufficient excitation for identification of the associated thermal dynamics. Furthermore, the experimental dataset covered the normal operating range of the PEMFC stack, including current levels up to 220 A and outlet coolant temperatures up to approximately 60 °C. Therefore, the identified models were developed and evaluated within the intended operating region of the fuel-cell system. The experimental dataset was divided into training and testing subsets using a 70/30 split. The first 70% of the data was used for N4SID model identification, while the remaining 30% was reserved for model validation. The testing region was intentionally selected from a different operating segment of the experiment to assess the generalization capability of the identified models. Although the validation data exhibit smaller variations than the identification dataset, they represent operating conditions not used during model estimation and therefore provide an independent assessment of prediction performance.

Different input configurations consisting of I, V, Tin, [I , V], [I, Tin], [V, Tin], [I, V, Tin] were selected and evaluated using both the base line and input delayed state-space virtual temperature prediction model. Prediction performance was evaluated on the testing dataset using the root mean square error (RMSE), ensuring an unbiased assessment of the model's generalization capability.

3. Results and discussion

This section evaluates N4SID-based virtual temperature models using different input configurations. Baseline and delay-optimized models are compared through the identified state-space parameters, outlet coolant temperature predictions, and RMSE values to assess the effectiveness of the proposed delay-aware approach.

3.1. State-Space Model Identification Results

Table 2 presents the state-space matrices identified using the baseline N4SID model for different input configurations without input delay. Although some identified A values are slightly greater than unity, the models remained bounded and produced accurate temperature predictions, consistent with the slow thermal dynamics of the PEMFC cooling system. The identified parameters vary considerably with predictor selection, indicating a strong influence of input variables on model dynamics and prediction performance. Table 3 presents the delay-optimized models. Compared with the baseline case, the identified parameters change significantly, showing that delayed inputs alter the dynamics captured by N4SID and improve the representation of PEMFC thermal-memory effects. The optimum delay for each configuration is also reported in Table 3.

Table 2: Matrices obtained for different combinations of input for baseline N4SID model

Input	A	B	C	D
I	1	7.7357×10^{-5}	0.7071	0
V	1	-4.7627×10^{-4}	-0.7071	0
T_{in}	1	1.4467×10^{-6}	-196.5259	0
[I, V]	0.9999	$[0.0716 \quad 0.9388] \times 10^{-3}$	0.7071	0
[I, T_{in}]	0.9984	$[-0.0002 \quad -0.0028]$	-0.7065	0
[V, T_{in}]	0.9982	$[0.3373 \quad -0.7928] \times 10^{-4}$	−34.7640	0
[I, V, T_{in}]	1	$[-0.0003 \quad -0.0053 \quad 0.0038]$	-0.7067	0

.

Table 3: Matrices obtained for different combinations of delay-optimized N4SID model

Input	A	B	C	D	Optimum Delay(s)
I	1.0001	-5.0526×10^{-7}	34.7640	0	3
V	1.0001	1.5910×10^{-6}	34.7640	0	2
T_{in}	1.001	-1.6308×10^{-7}	34.7640	0	2
[I, V]	0.9999	$[-0.0759 \quad -0.9756] \times 10^{-3}$	-0.7071	0	2
[I, T_{in}]	0.9990	$[-0.0061 \quad -0.1707] \times 10^{-4}$	-78.4409	0	2
[V, T_{in}]	0.9973	$[-0.1665 \quad 0.3814] \times 10^{-4}$	109.8847	0	5
[I, V, T_{in}]	1.0012	$[-0.0269 \quad -0.5004 \quad 0.3939] \times 10^{-4}$	-70.2064	0	4

3.2. Comparison of prediction performance

Figure 5 presents the prediction performance of the baseline and delay-optimized N4SID models corresponding to the test region (virtual sensing) shown in Figure 4. The measured and predicted outlet coolant temperatures were plotted considering the baseline and delay-optimized N4SID models for different input configurations.

The results show that input-delay optimization reduced the prediction error for all investigated input configurations.

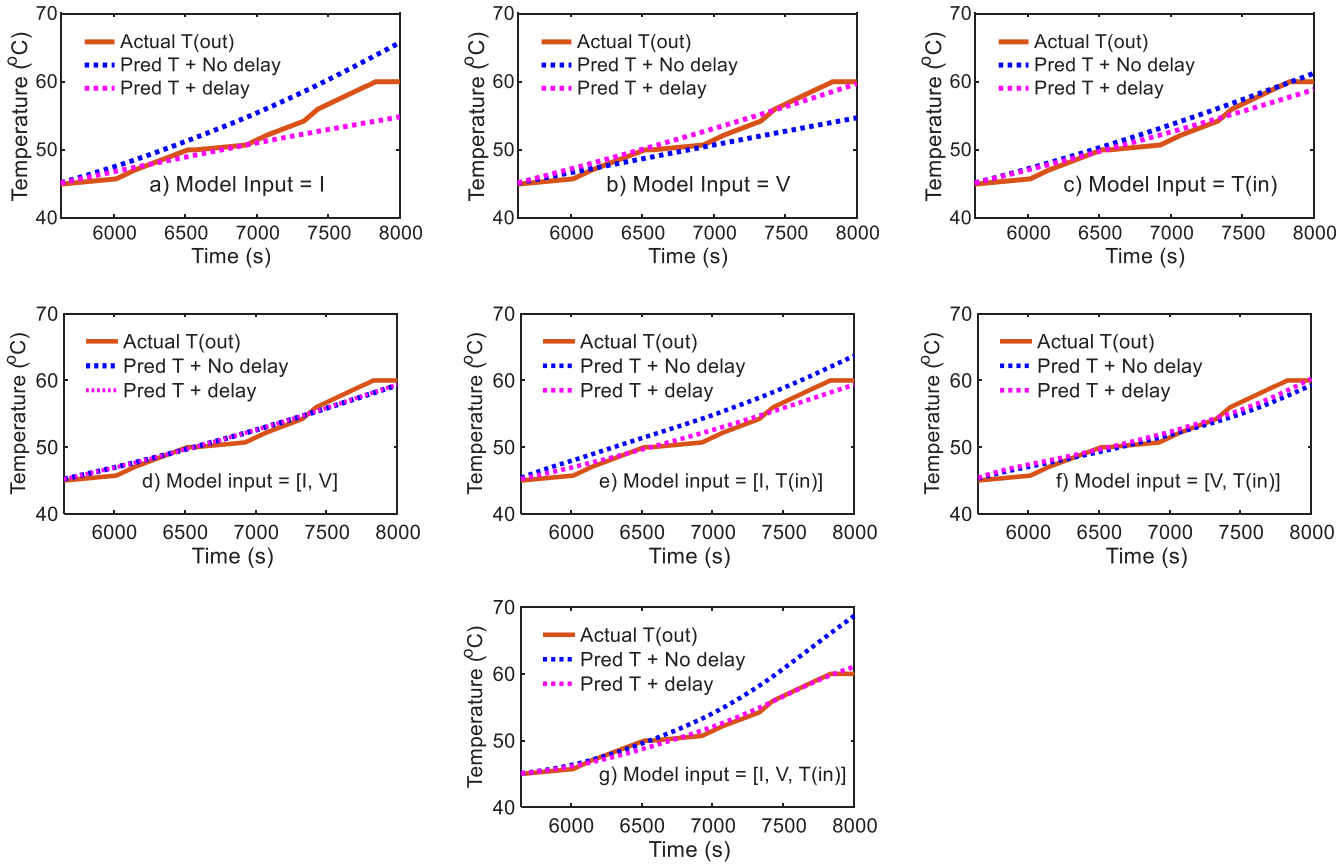


Figure 5: Measured and predicted outlet coolant temperature using baseline and delay-optimized N4SID models for different input configurations.

Table 4 summarizes the RMSE values obtained for the investigated input configurations.

Table 4: Effect of input delay on RMSE of various input configurations

Model Input	RMSE		Optimum Delay(s)
	No Delay	Delay	
I	3.0651	2.5285	3
V	2.6557	1.0415	2
T_{in}	1.2729	1.0532	2
[I, V]	0.8997	0.8772	2
[I, T_{in}]	2.3674	1.3671	2
[V, T_{in}]	1.0742	0.9036	5
[I, V, T_{in}]	3.2399	0.5112	4

In Fig. 5(a), where stack current was used as the only model input, the RMSE decreased from 3.0651 °C to 2.5285 °C after introducing a 3-s input delay. Although the improvement is moderate, the delayed model reduces the overprediction observed in the baseline response, indicating that current alone does not fully describe the thermal behaviour of the system. In Fig. 5(b), voltage as the sole input produced a stronger improvement, with the RMSE decreasing from 2.6557 °C to 1.0415 °C after applying a 2-s input delay. This suggests that voltage contains useful electrochemical information related to heat generation and responds more closely to the thermal evolution of the stack than current alone.

For Fig. 5(c), the RMSE decreased from 1.2729 °C to 1.0532 °C with a 2-s delay, indicating a modest improvement because inlet temperature is already directly related to outlet temperature. For the combined input cases, Fig. 5(d) shows that the [I, V] configuration gave the best baseline performance, with an RMSE of 0.8997 °C, and improved slightly to 0.8772 °C with a 2-s delay. This suggests limited additional benefit from delay optimization. In Fig. 5(e), the [I, Tin] configuration improved from 2.3674 °C to 1.3671 °C with a 2-s delay, showing that combining current with delayed inlet temperature better captures thermal boundary effects. In Fig. 5(f), the [V, Tin] configuration improved from 1.0742 °C to 0.9036 °C with a 5-s delay, confirming that voltage and inlet temperature provide complementary electrochemical and cooling-boundary information. The strongest improvement was obtained in Fig. 5(g), where the [I, V, Tin] configuration reduced RMSE from 3.2399 °C to 0.5112 °C with a 4-s delay.

This result shows that delay optimization improves alignment between inputs and thermal response.

It is important to note that the optimum delays of 2–5 s utilised are not the overall thermal response time of the PEMFC cooling system. This is confirmed by Jian et al. (2018)

who noted that a process can indeed exhibit a short dead time while requiring a much longer period to reach steady state. Hence, the optimized delays mainly represent the effective lag between changes in the predictor variables and the first observable effect on outlet coolant temperature. Overall, these results confirm that delayed inputs capture PEMFC thermal-memory effects and significantly improve state-space virtual temperature prediction.

4. Conclusion

This study investigated the influence of predictor-variable selection and input-delay optimization on N4SID-based virtual temperature sensing in a PEM fuel cell. Multiple input configurations were evaluated. The results demonstrated that incorporating delayed inputs consistently improved prediction accuracy by capturing thermal-memory effects within the cooling system. Among the investigated configurations, the combination of current, voltage, and inlet coolant temperature with delay optimization achieved the best performance, reducing the RMSE from 3.2399 °C to 0.5112 °C. The proposed delay-aware state-space modelling approach provides an effective and computationally efficient framework for PEMFC virtual temperature prediction and fault-tolerant monitoring applications. Future work will investigate the robustness of the proposed delay-aware virtual sensing framework under different operating conditions, load profiles, and thermal-management strategies.

Acknowledgments

This work has been partially carried out thanks to the support of (1) Grant Ref: PID2020-116616RB-C31 and (2) Triple-M Ref.: EPIT0872023-UHU.

References

Deng, Z., Miao, B., Cui, Y., Chen, J., Pan, Z., Liu, H., Deendarlianto, D., Suwarno, S., Chan, S.H., 2025. Towards high-performance fuel cell systems: Comprehensive review of methods for modeling, control, and optimization. Renewable and Sustainable Energy Reviews 224, 116122. https://doi.org/10.1016/j.rser.2025.116122

Drakunov, S.V., Perruquetti, W., Richard, J.-P., Belkoura, L., 2006. Delay identification in time-delay systems using variable structure observers. Annual Reviews in Control 30, 143–158. https://doi.org/10.1016/j.arcontrol.2006.08.001

Fuchs, B., Altmann, F., Vrlić, M., Braun, S., Kozek, M., Hametner, C., Jakubek, S., 2025. Nonlinear distributed-parameter observer design for efficient estimation of internal temperature profiles in polymer electrolyte membrane fuel cells. Nonlinear Dyn 113, 18265–18289. https://doi.org/10.1007/s11071-025-11108-0

Huynh, T.N., Ahn, C., Hong, K.W., Kwon, Y.R., Lee, J., Yu, W., Cho, G.Y., Kim, J.-G., 2026. Developing a real-time internal temperature monitoring framework for a polymer electrolyte membrane fuel cell. Applied Thermal Engineering 300, 131381. https://doi.org/10.1016/j.applthermaleng.2026.131381

Ingebretsen, J., Rotondo, D., 2022. An improved delay and state observer for SISO LTI systems with known delay lower bound. Presented at the 63rd International Conference of Scandinavian Simulation Society, SIMS 2022, Trondheim, Norway, September 20-21, 2022, pp. 353–358. https://doi.org/10.3384/ecp192050

Jian, Q., Huang, B., Luo, L., Zhao, J., Cao, S., Huang, Z., 2018. Experimental investigation of the thermal response of open-cathode proton exchange membrane fuel cell stack. International Journal of Hydrogen Energy 43, 13489–13500. https://doi.org/10.1016/j.ijhydene.2018.05.097

Li, X., Xu, H., Ming, P., Liu, Y., Ma, C., Tian, S., Liu, D., Cheng, Z., Shi, X., 2026. Short-term multi-step temperature prediction for automotive fuel cells via focus-time calibration model. Energy Conversion and Management 348, 120597. https://doi.org/10.1016/j.enconman.2025.120597

Liu, J., Liu, Y., Zhao, P., Yan, F., Zheng, H., Wu, Y., Lu, C., 2025. Fuel Cell Thermal Management System Based on Model Predictive Control, in: 2025 5th International Conference on New Energy and Power Engineering (ICNEPE). Presented at the 2025 5th International Conference on New Energy and Power Engineering (ICNEPE), IEEE, Guangzhou, China, pp. 965–971. https://doi.org/10.1109/ICNEPE67923.2025.11384135

MathWorks, 2026. System Identification Toolbox User's Guide. The MathWorks, Inc., Natick, Massachusetts, USA.

Novella-Rodrìguez, D.F., Witrant, E., Muro-Cuéllar, B.D., Márquez-Rubio, J.F., 2019. Adaptive Multi-Observer Design for Systems with Unknown Long Input Delay. IFAC-PapersOnLine 52, 37–42. https://doi.org/10.1016/j.ifacol.2019.12.203